HEDL-SA-1833-FP

CONF-791045--6

A PHYSICALLY BASED MODEL FOR HELIUM RELEASE FROM IRRADIATED BORON CARBIDE

C. E. Beyer
G. W. Hollenberg
S. A. Duran

The American Ceramic Society
October 14-17, 1979
New Orleans, LA

HANFORD ENGINEERING DEVELOPMENT LABORATORY
Operated by Westinghouse Hanford Company, a subsidiary of Westinghouse Electric Corporation, under the Department of Energy Contract No. EY-76-C-14-2170

DISCLAIMER

HEDL-SA-1833

A PHYSICALLY BASED MODEL FOR HELIUM RELEASE FROM IRRADIATED BORON CARBIDE

By

C. E. Beyer
G. W. Hollenberg
S. A. Duran

ABSTRACT

The model is based on the nucleation of nonequilibrium helium bubbles under high pressures. The bubbles subsequently act as traps and grow as the result of gas atom diffusion. Model predictions are compared with bubble densities, sizes, and helium release characteristics of irradiated boron carbide.

A PHYSICALLY BASED MODEL FOR HELIUM RELEASE FROM IRRADIATED BORON CARBIDE

By

C. E. Beyer
G. W. Hollenberg
S. A. Duran

I. INTRODUCTION

Boron Carbide (B_4C) is the internationally accepted absorber material for control rods in fast breeder reactors. When boron carbide absorbs neutrons, lithium and helium are produced:

$$^{10}B + {}^{1}n \rightarrow {}^{7}Li + {}^{4}He$$

The helium apparently has insignificant solubility within the boron carbide matrix, creating two potential problems in absorber pin design. Helium can diffuse to a free surface and escape as a gas, leading to a buildup in pin plenum pressure; or the helium atoms can precipitate as small bubbles within the matrix, leading to boron carbide pellet swelling. Both helium release and pellet swelling limit the lifetime of absorber pins since either can lead to excessive stress in the cladding.

The Hanford Engineering Development Laboratory (HEDL) has conducted extensive in-reactor testing[1,2,3] of boron carbide in support of the fast breeder reactor program. The data from these tests have been used to develop empirical correlations for both gas release[4] and swelling.[5] Typical gas release data as a function of burnup at various temperatures are shown in Figure 1. The release data typically shows two distinct regions of release, a primary region with a high release rate early-in-life, and a secondary release region at a much lower release rate later-in-life. Past observations[5] have shown that B_4C swelling is roughly proportional to the gas retained in the irradiated material; and consequently, inversely related to helium release.

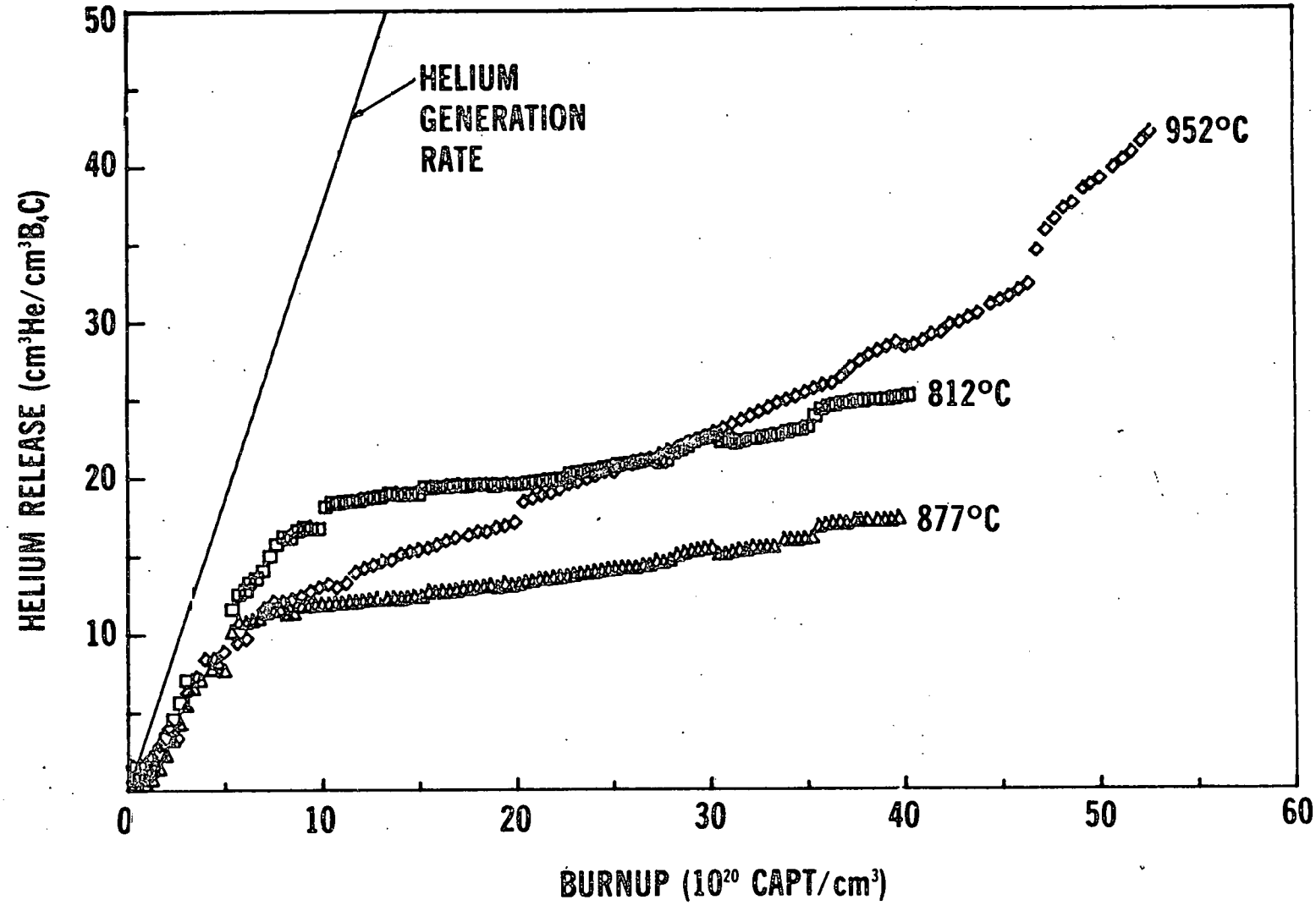

FIGURE 1. Helium Release from Boron Carbide.

There have been no previous attempts to develop a physically based model describing gas release or swelling specifically for boron carbide. The purpose of this work has been to utilize simple diffusion theory and microstructural observations to produce a relatively simple physical model for describing helium release from irradiated boron carbide. The model is not a fully comprehensive theoretical one, but is a basis for further development.

Much effort has been expended in describing gas release from oxide fuel and this vast knowledge of physical behavior provided a base for describing gas release from boron carbide. A schematic of the physical phenomena affecting gas release from oxide fuels is shown in Figure 2. There are, however, important differences in boron carbide versus oxide fuel gas release behavior. The main differences are due to the nonequilibrium nature of the bubbles and their lack of mobility in boron carbide at normal operating temperatures (i.e. < 1250°C). In contrast, the bubbles in oxide fuels are in mechanical equilibrium with the matrix and somewhat mobile. Inert gases in metals have also been studied with great interest, particularly in fast neutron reactors. However, in most cases these bubbles are also in mechanical equilibrium with their matrix, and consequently these models do not directly apply to boron carbide.

Since the irradiated boron carbide microstructure plays an important role in helium release it is appropriate to review some past observations. The microstructure of irradiated samples has been characterized through the use of transmission electron microscopy (TEM). Small plate-like bubbles with large strain fields surrounding them on the {110} or {111} rhombohedral planes have been observed, Figure 3, by several investigators.[6-12] The conclusion of these investigators has been that the bubbles exist under extremely high pressures and thus are not in mechanical equilibrium with the matrix. Postirradiation annealing of these samples reveals that temperatures of 1400 to 1600°C are needed to relieve the strain fields and obtain an equilibrium bubble. Many of these investigators observed zones completely denuded of bubbles adjacent to the grain boundaries. A typical example is shown in Figure 4.

MODELING FOR FUEL

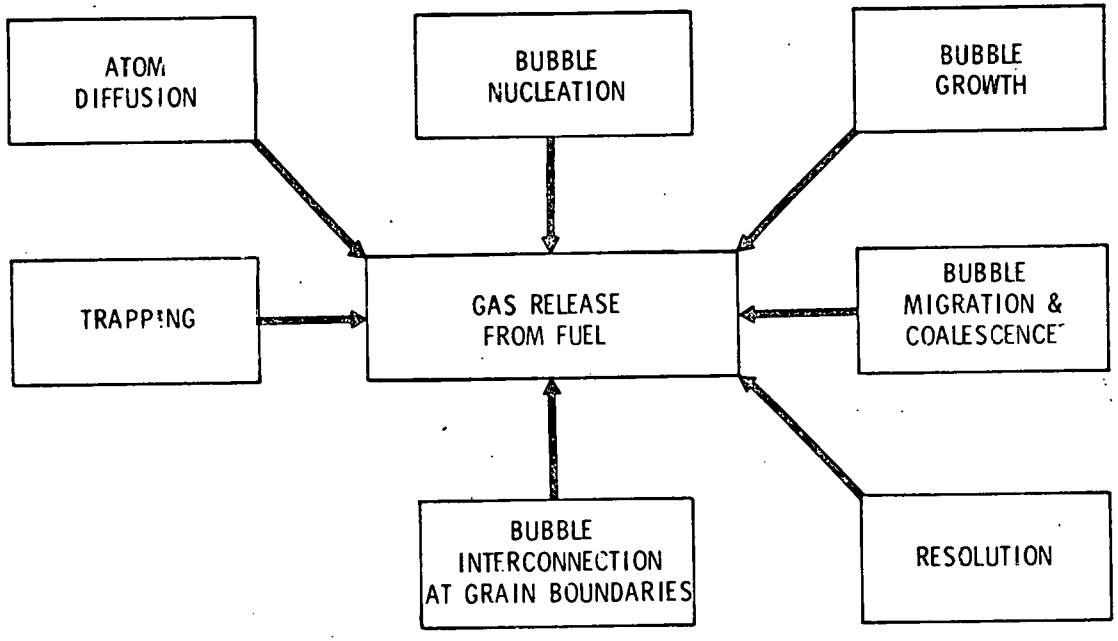

FIGURE 2. Modeling for Fuel.

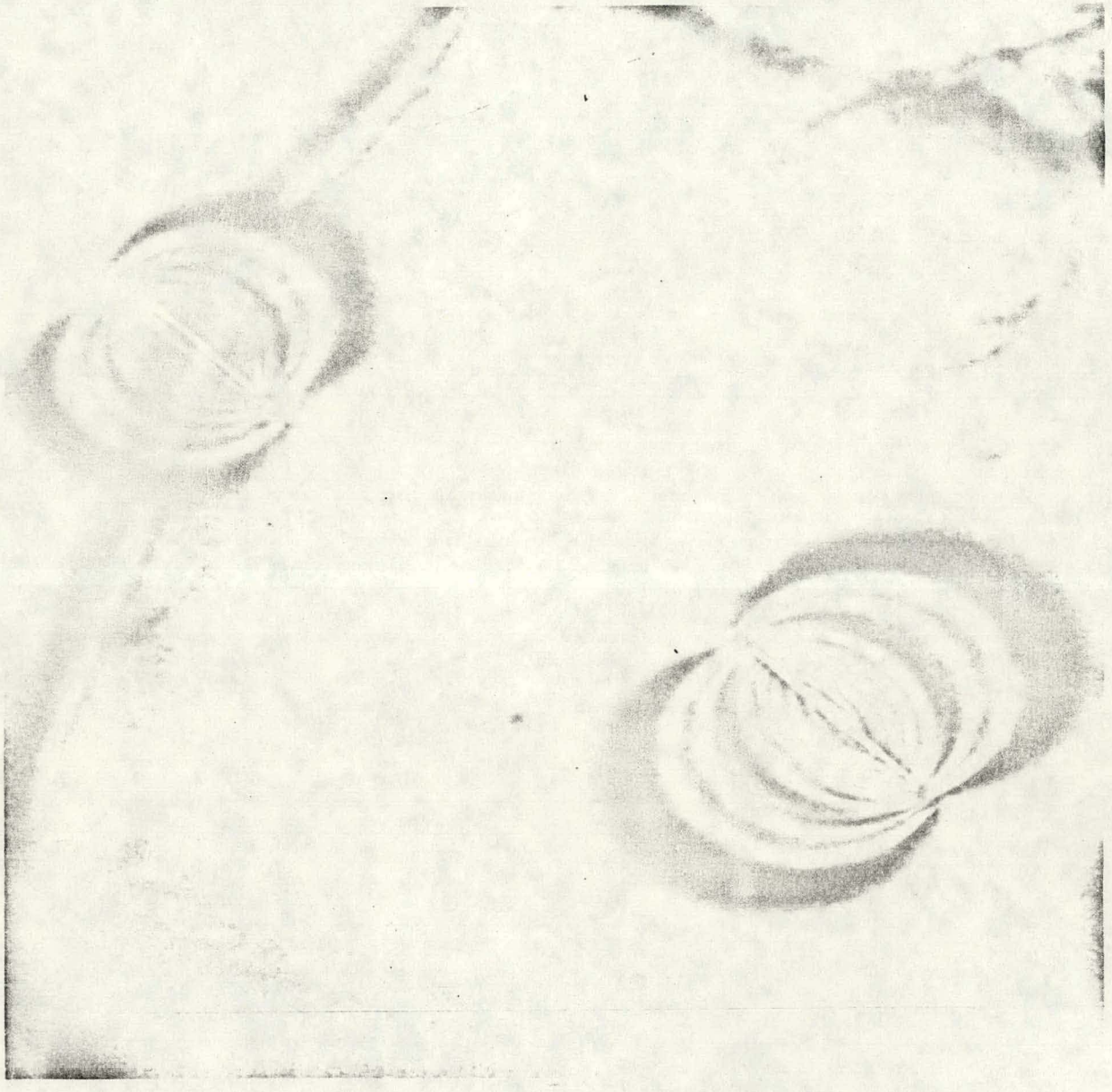

HEDL 7901-186.13

FIGURE 3. High Pressure Helium Bubbles In Irradiated Boron Carbide.

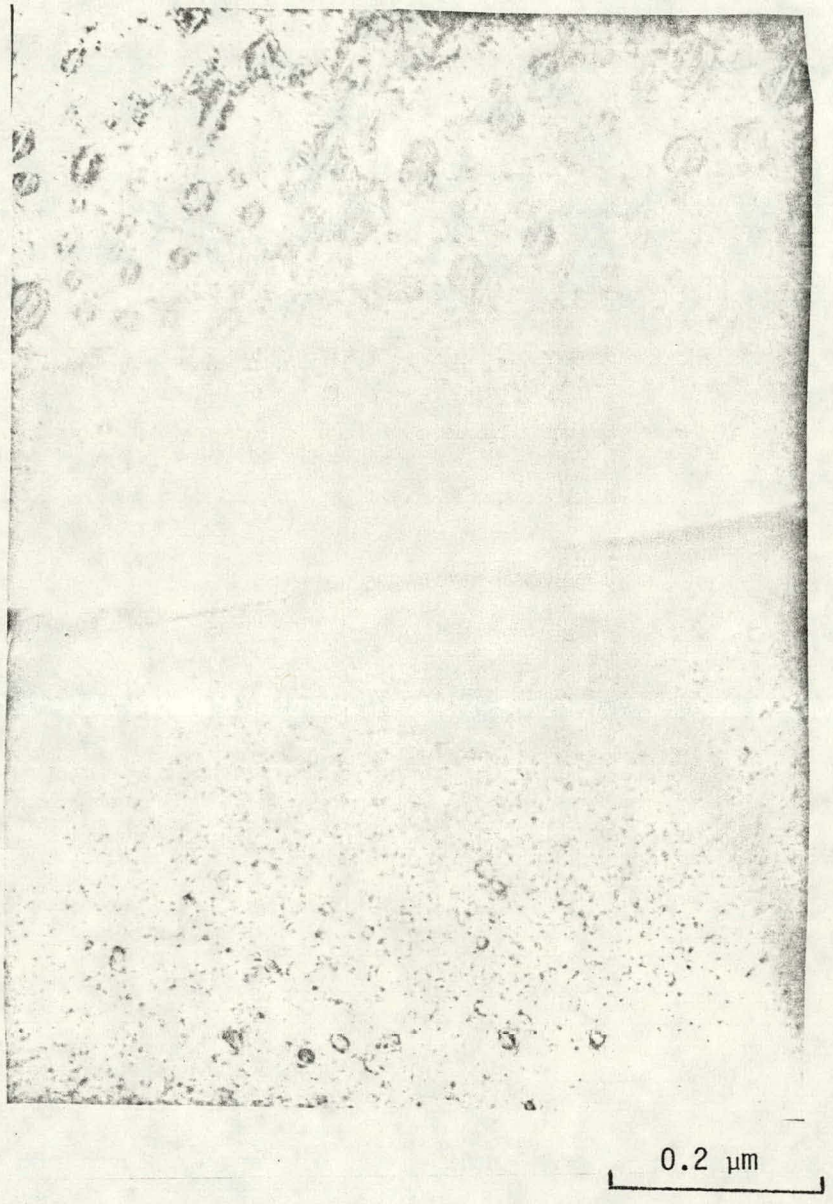

FIGURE 4. Denuded Grain Boundary in Irradiated Boron Carbide.

Bubble densities and diameters have been quantitatively characterized by Hollenberg and Mastel.[13] Their data was taken from samples with a wide range of irradiation temperatures. These microstructural data along with gas release data will be compared against the model's predictions.

II. MODEL DESCRIPTION

The model is divided into two parts which treat the primary and secondary release regions as indicated by the release curves shown in Figure 1. The primary release, GR_p, takes into account diffusional release early-in-life before bubble nucleation has been initiated. With the absence of bubbles to trap the diffusing gas, the diffusional release is modeled by assuming the grains are equivalent to spherical particles, Figure 5a, all of equal size:

$$GR_p(t_p) = \dot{F}t_p - \frac{\dot{F}r_g^2}{15\,D_{He}} + \frac{6\,\dot{F}r_g^2}{\pi^4\,D_{He}} \sum_{n=1}^{\infty} \frac{e^{-n^2\pi^2 D_{He}/r_g^2}}{n^4} \qquad \text{Eq. 1}$$

where $GR_p(t_p)$ = primary gas release at time t_p, cm^3He/cm^3B_4C

t_p = time for primary release, sec.

$\dot{F}$ = ^{10}B reaction rate

r_g = grain radius

D_{He} = helium diffusion coefficient in boron carbide

The grain boundaries are assumed to be free surfaces for release. Booth[14] was the first to develop this equivalent sphere model for gas release and it has been used extensively as a simple model for gas release from fuel.[15] The activation energy for diffusion in this model was taken from Clayton, et al.,[16] who measured helium release from very lightly irradiated boron carbide (< $2x10^{20}$ captures/cm^3):

$$D_{He} = 4.4x10^{-9}\, e^{-2900/RT} \qquad \text{Eq. 2}$$

where D_{He} = helium diffusion coefficient, cm^2/sec

R = gas constant, 1.987 cal/°K-mole

T - temperature, °K.

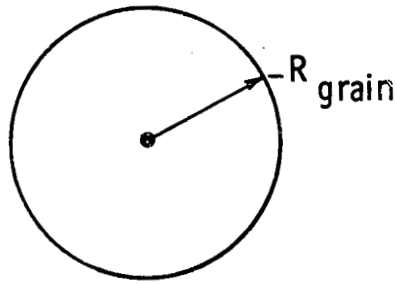

- DIFFUSION FROM GRAIN
- EQUIVALENT-SPHERE (BOOTH) MODEL

FIGURE 5a. Primary Release Model.

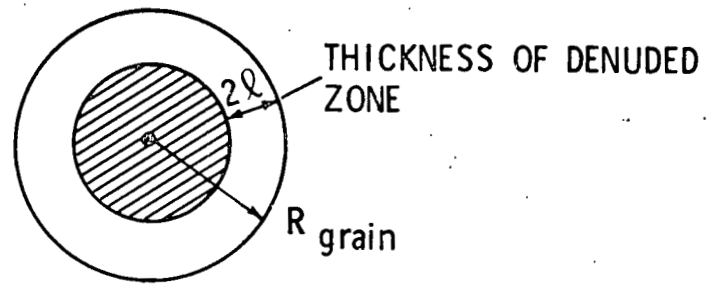

- DIFFUSION FROM DENUDED ZONE
- $\ell << R$ GRAIN

FIGURE 5b. Secondary Release Model.

HEDL 7908-263.1

However, the pre-exponential term was decreased by a factor of 4 to obtain better agreement with the observed gas release, bubble density and bubble diameter data.

As the irradiation proceeds bubble nucleation is initiated, which is the transition point to the secondary region of release (GR_S). The bubbles are assumed to be stationary because their nonequilibrium shape and high stresses in the immediate vicinity of the bubble make their movement energetically very difficult. Consequently, the bubbles act as traps for the diffusing gas. At temperatures below 1100°C the bubble density is relatively high, 10^{17} to 10^{18} bubbles/cm^3, so that all the gas produced within the interior of the grain is trapped and only that gas produced in the zone denuded of bubbles adjacent to the grain boundary is available for diffusional release, Figure 5b. The denuded zone width, defined here as 2ℓ, is proportional to the diffusion distance between bubbles in the grain matrix.

A steady-state nucleation model first proposed by Turnbull[17] and later derived and integrated by Speight[18] was used to predict instantaneous formation of bubbles. The density, N, of stationary bubbles for temperatures below 1100°C becomes:[18]

$$N = \frac{(\pi)^{0.5}\ \alpha\ \dot{F}\ R_o^2}{2D_{He}\ BC + B\mu\ \dot{F}\ R_o} \left[\frac{e^S\ \mathrm{erfc}(S)^{0.5}}{(S)^{0.5}} \right] \qquad \text{Eq. 3}$$

Where N = bubble density, bubbles/cm^3

$S = \dfrac{\pi\ \dot{F}\ \mu\ R_o^4}{2\ D_{He}\ BC}$

α = bubbles created per reaction

R_o = critical radius for nucleation, cm

B = Van Der Walls' Gas Constant

C = concentration of solute helium atoms, atom/cm^3

μ = helium track, cm

with the remaining variables as defined for Equation 1.

Bubble growth was treated using a differential equation developed by Greenwood, Foreman, and Rimmer[19] for nonequilibrium bubbles at high pressures.

$$\frac{dR}{dt} = \frac{A_1 t}{R^4} - \frac{A_2}{R^2} \qquad \text{Eq. 4}$$

where R = bubble radius
A_1 = $3\Omega 2\ D_V C_V\ \dot{F}/4\pi N$
A_2 = $2\gamma\Omega^2$ DvCv/KT
t = time, sec.
K = Boltzmann's Constant
T = temperature, °K
γ = surface tension, 1000 dyne/cm
Ω = helium atomic volume, 5.2×10^{-25} cm^3
D_V = vacancy diffusion coefficient
C_V = vacancy concentration

In their solution[19] the bubble pressure was assumed to be only slightly greater than the equilibrium pressure. However, bubbles within irradiated B_4C are expected to be at pressures significantly greater than the equilibrium pressure. Hence, it was necessary to numerically integrate the differential expression of Greenwood, et al.[19] to obtain the bubble size.

Since the denuded zone thickness, 2ℓ, is much smaller than the radius of the grain, the solution for diffusion through a flat plate of thickness 2ℓ was used for calculating the secondary release. However, the spherical geometry was retained in calculating the internal surface area of the grains. The release was integrated

from the end of the primary release, t_p, to the total irradiation time of interest, t_F.

$$GR_S(t_F) = \frac{3\dot{F}\ell}{r_g}(t_F - t_p) + \frac{96\dot{F}\ell^3}{\pi^4 D_{He} r_g}\left\{\sum_{n=0}^{\infty}\frac{1}{(2n+1)^2}\left[e^{-(2n+1)^2\pi^2\beta t_F} - e^{-(2n+1)^2\pi^2\beta t_p}\right]\right\}$$

where $GR_S(t_F)$ = secondary release at t_F, cm^3/cm^3 B_4C

ℓ = half the denuded zone thickness

β = $D_{He}/4\ell^2$

t_F = total irradiation time of interest, sec

with the remaining variables as defined for previous equations.

A summary of the material parameters and the values used in the above models is presented in Table 1.

III. MODEL PREDICTIONS COMPARED TO DATA

Three experimentally measured parameters were compared against the models' predictions. They are observed helium release, bubble density and bubble diameter.

In-reactor helium release has been monitored insitu by two EBR-II instrumented tests, BICM-1[2] and BICM-2,[3] with pressure sensors. Figures 6 through 9 compare model predictions to the measured releases as a function of burnup for the range of temperatures covered by these two experiments. These figures also show the helium generation rates. In these figures, helium release is in units of cm^3 of helium per cm^3 of boron carbide and burnup is ^{10}B neutron captures per cm^3 of boron carbide. Release at the lowest irradiation temperature of 700°C (B_4C centerline), Figure 6, shows that the model slightly underpredicts the primary release and agrees very well with the secondary region. At 812°C,

TABLE 1

MATERIAL PARAMETERS REQUIRED FOR
BORON CARBIDE GAS RELEASE MODEL

	Parameters	Value	Reference
R_o,	critical radius for nucleation	5×10^{-8} cm	20
γ,	surface tension for B_4C	1000 dyne/cm	21
Ω,	helium atomic volume	5.2×10^{-25} cm^3	22
α,	bubbles created per reaction	5	20
β,	Van Der Walls' Gas constant for helium	3.885×10^{-23}	23
μ,	helium track distance	4.72×10^{-4} cm	24
Q_{He},	helium activation energy for diffusion	29,000 cal/mole	16
D_o,	pre-exponential term for helium diffusion coefficient equation.	4.4×10^{-9}	*

* Selected to obtain agreement between the predictions and the data.

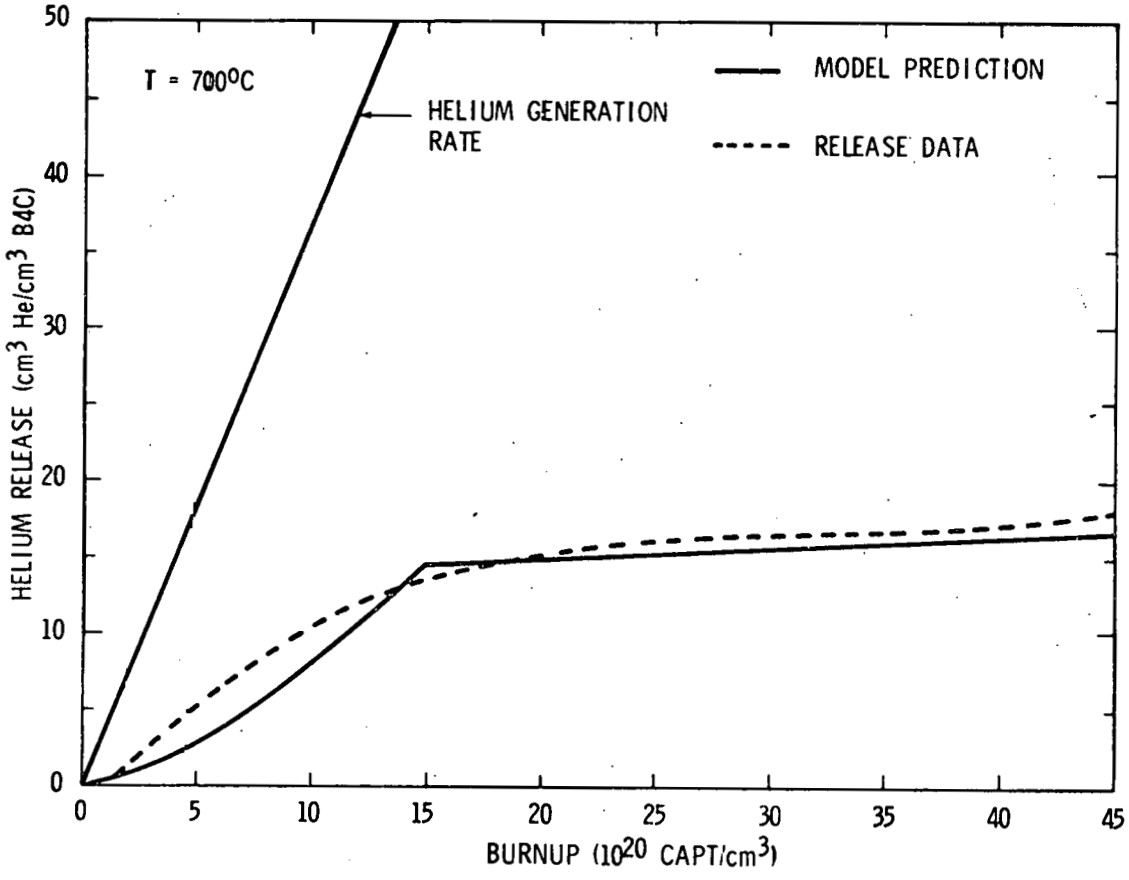

FIGURE 6. Comparison of Predicted to Measured Release at 700°C.

Figure 7, the model also slightly underpredicts release in the primary region but agrees very well for the secondary release. At 877°C, Figure 8, the model agrees very well for the primary region but overpredicts the release rate slightly for the secondary region. The highest irradiation temperature of 952°C, Figure 9, shows good agreement for the primary region and a very slight overprediction in release rate for the secondary region.

The model predicts the shape of the helium release from boron carbide quite well. Of particular interest in Figures 6 and 8 is the curvature at very low burnups (i.e., $< 3 \times 10^{20}$ captures/cm^3) which is in agreement with the diffusional release from an individual grain. The model's transition from long-range diffusion of helium out of a grain to diffusion limited by trapping, i.e., the change from primary to secondary is very abrupt. The actual data, however, show a more gradual transition between the two release regions, perhaps reflecting the statistical character of the nucleation process.

The agreement of release rates in the secondary region is quite good between the model and the actual data. At higher burnup levels ($> 50 \times 10^{20}$ captures/cm^3) matrix damage (such as microcracking) due to irradiation is expected to limit the extrapolation of this model. Microcracking may be extensive enough to affect the amount of free surface for release.

Hollenberg and Mastel[13] have quantitatively characterized bubble densities and diameters from boron carbide samples irradiated over a wide range of temperatures (540°C to 1820°C). A comparison of their measured values with those predicted by the model is shown in Figures 10 and 11. The model agrees favorably with the density data, Figure 10, below 1000°C with a slight underprediction. However, the underprediction is within the estimated scatter in the data. A significant overprediction by the model is observed for the two high temperature samples of 1600 and 1850°C. This may be the result of bubble coalescence and/or migration taking place at these temperatures. These phenomena are not treated by the current model. Hollenberg and Mastel have also noted that the bubbles at these high temperatures appear to be in mechanical equilibrium (i.e., no strain fields and equiaxed in shape)

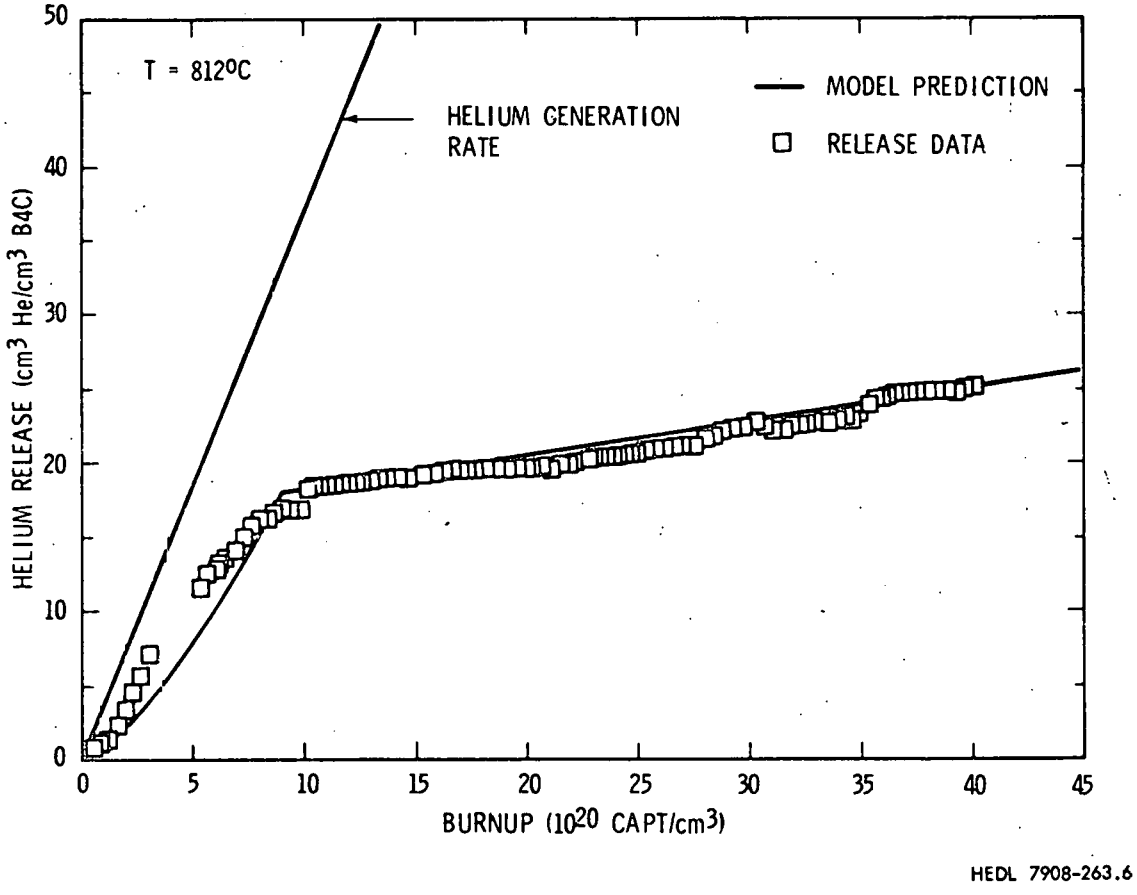

FIGURE 7. Comparison of Predicted to Measured Release at 812°C.

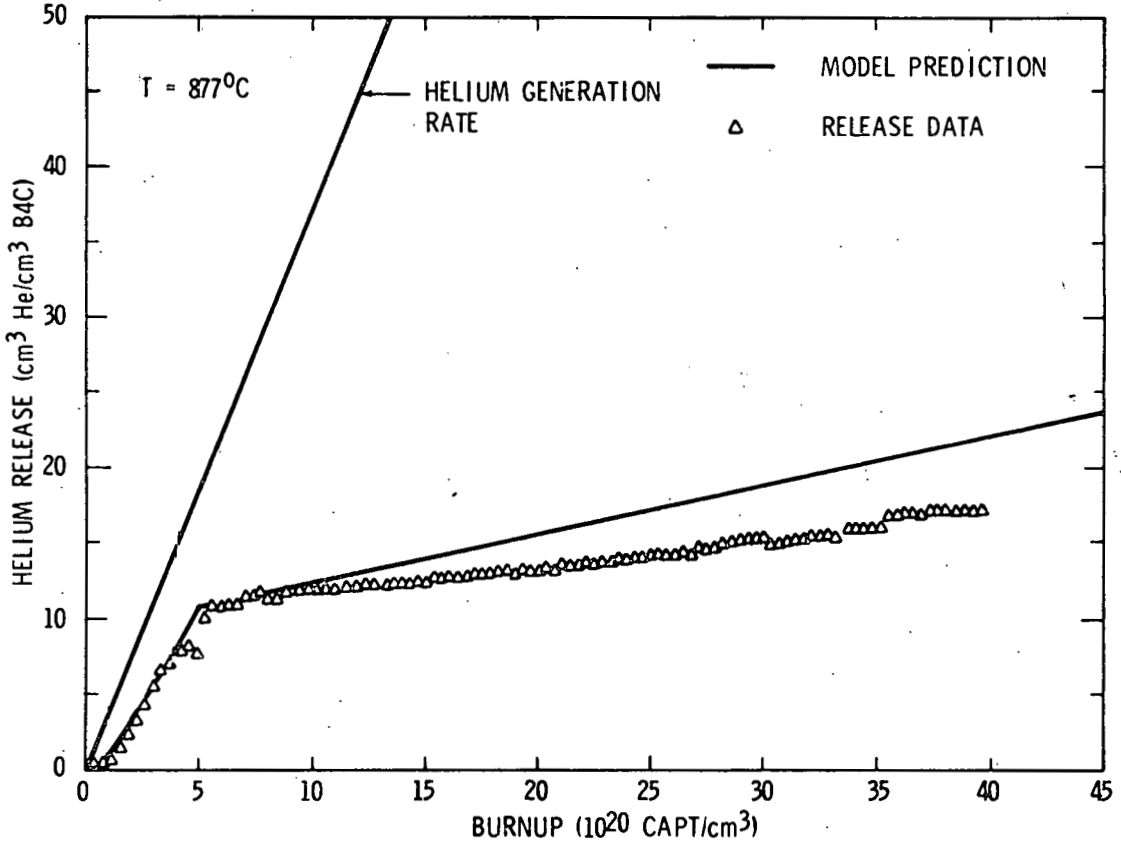

FIGURE 8. Comparison of Predicted to Measured Release at 877°C.

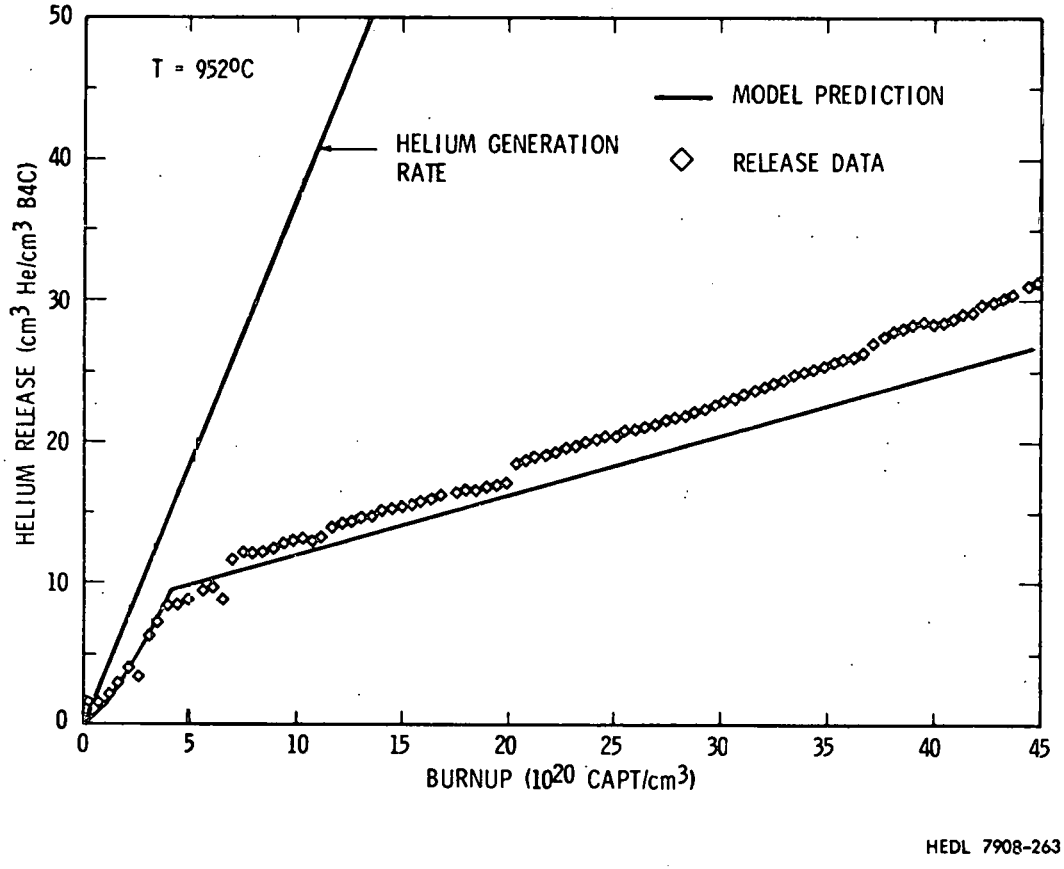

FIGURE 9. Comparison of Predicted to Measured Release at 952°C.

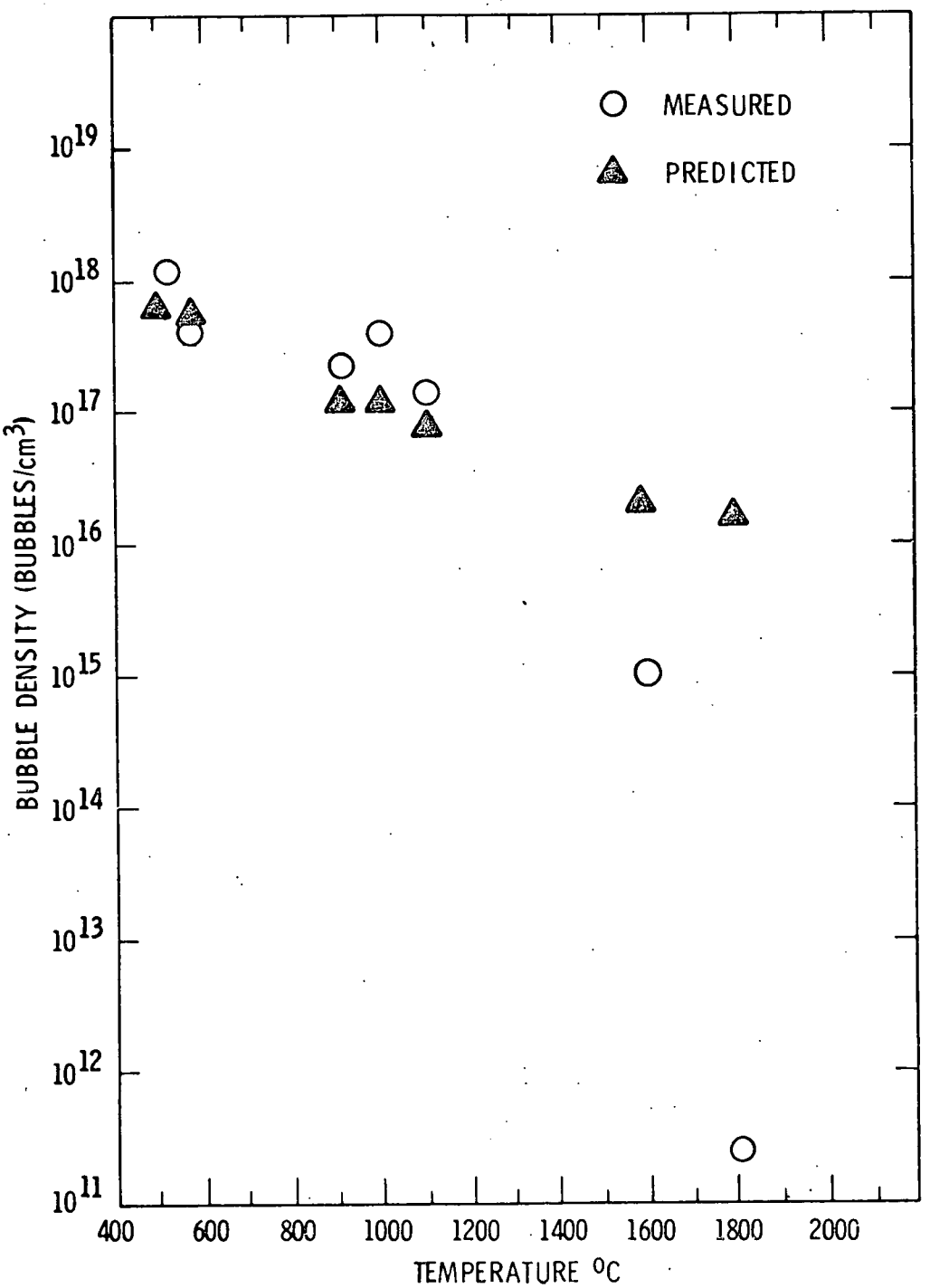

HEDL 7903-043.1

FIGURE 10. Comparison of Model Prediction to Measured Bubble Density versus Irradiation Temperature.

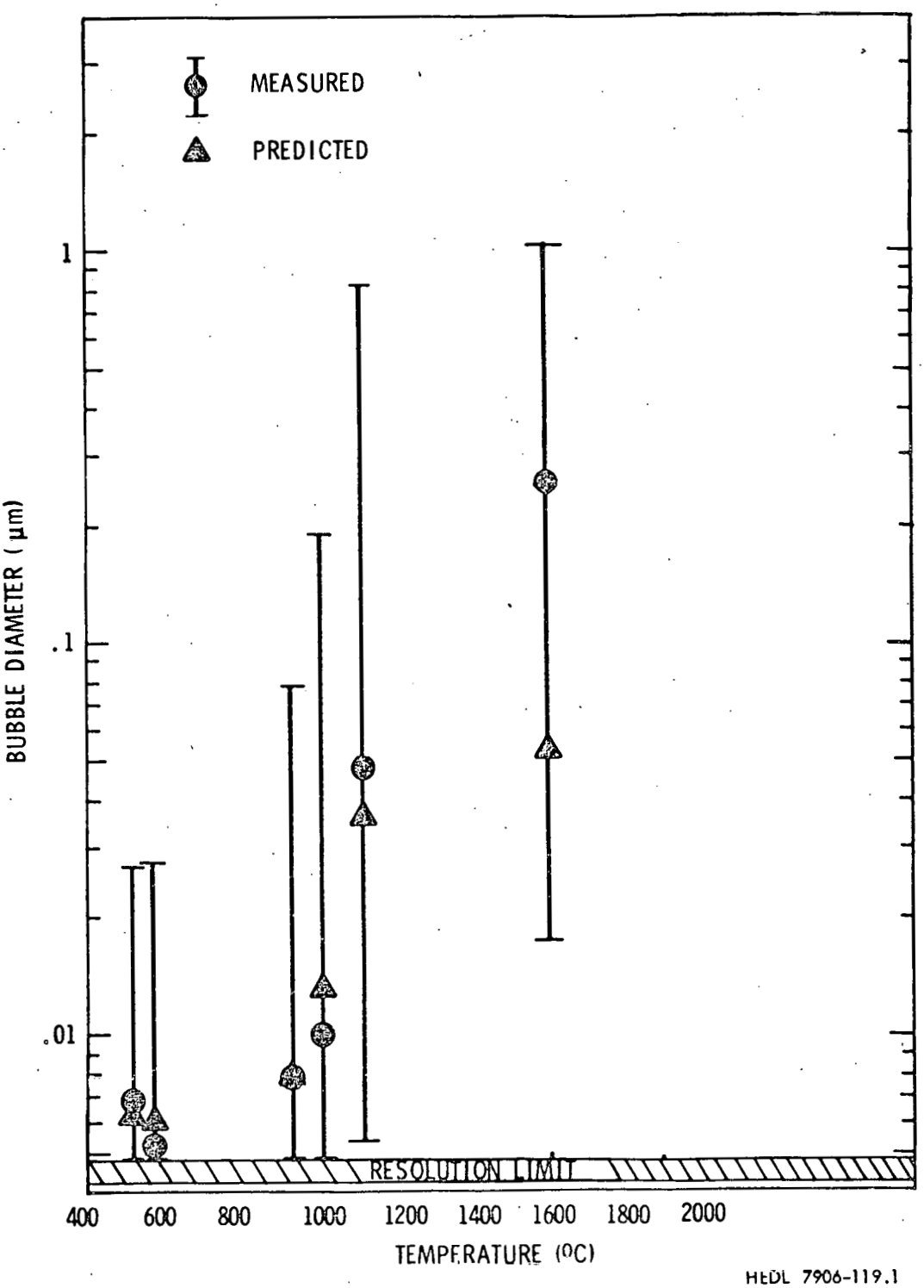

FIGURE 11. Comparison of Model Predictions to Measured Bubble Diameter Versus Irradiation Temperature.

and heterogeneously distributed in the matrix. From this they concluded that the bubbles may be heterogeneously nucleated at strong trapping sites such as grain boundaries, dislocations and twin boundaries: another potential explanation of the lack of agreement at high temperatures.

A comparison of the model predictions with the measured bubble diameter, Figure 11, below 1100°C shows good agreement. As with the density, a significant underprediction is seen at high temperatures, 1600°C. This underprediction is most likely related to the problems discussed above for the differences in measured and predicted densities for these samples.

IV. CONCLUSIONS

Overall, the model adequately predicts helium release in the temperature and burnup ranges of 500 to 1100°C and 0 to 50×10^{20} captures/cm^3, respectively. In particular, it indicates that the modeling of release from individual grains explains the primary release, and that release from the denuded zones adjacent to the grain boundaries adequately explains secondary release. Predictions of the model also agree with measured bubble density and diameter below $\sim$ 1100°C, but both are substantially underpredicted above this temperature range.

The areas in which limitations of the model exist and additional work that may improve the model are:

Limitations	Additional Work
• Material parameters used in the model.	• Additional data is needed to better define these parameters.
• Bubble nucleation and growth models at temperatures > 1100°C.	• Bubble migration, coalescence and and heterogeneous nucleation at strong trapping sites need to be treated.
• Release at burnups > 50×10^{20} captures/cm^3.	• Examine release and microstructure at high burnups to determine if damage influences the release.
• Transition point between primary and secondary release.	• Closer examination of both release and microstructure may give clues to how this may be physically modeled.

V. REFERENCES

1. J. A. Basmajian, et al., "Irradiation Effects in Boron Carbide Pellets Irradiated in Fast Neutron Spectra," Nucl. Tech., 16, p. 238, (1972).

2. A. L. Pitner, "Instrumented Fast Reactor Irradiation of Boron Carbide Pellets," Nucl. Tech., 30, p. 77 (1976).

3. G. W. Hollenberg, J. L. Jackson and J. A. Basmajian, The BICM-2 Instrumented Neutron Absorber Experiment, HEDL-TME 78-103, (1979).

4. J. A. Basmajian and A. L. Pitner, "A Correlation for Boron Carbide Helium Release in Fast Reactors," Trans. Am. Nucl. Soc., Vol. 26, p. 174 (June 1977).

5. J. A. Basmajian and A. L. Pitner, "Helium Retention and Its Effects on Boron Carbide Irradiated in a Fast Reactor," American Ceramic Society Bulletin, 54 [9] p. 826 (1975).

6. W. V. Cummings, J. J. Laidler, D. E. Mahagin, and B. Mastel, "Microstructure of Fast-Reactor-Irradiated Boron Carbide," Trans. ANS, 15, [2] p. 742, (1972).

7. G. L. Copeland, R. G. Donnelly, and W. R. Martin, "Irradiation Behavior of Boron Carbide," Nucl. Tech., 16 [1], pp. 226-37, (1972).

8. A. Jostsons and C. K. H. DuBose, "Microstructure of Boron Carbide After Fast Neutron Irradiation," J. Nucl. Mat., 44 [1], pp. 91-95, (1972).

9. K. H. G. Ashbee, "Defects in Boron Carbide, Before and After Neutron Irradiation," Acta, Met., 19 [10], pp. 1070-85, (1971).

10. A. Jostsons, C. K. H. DuBose, G. L. Copeland, and J. O. Stiegler, "Defect Structure of Neutron-Irradiated Boron Carbide," J. Nucl. Mat., 49 [2], pp. 136-50, (1973).

11. G. W. Hollenberg and W. V. Cummings, "Effect of Fast Neutron Irradiation on the Structure of Boron Carbide," J. Am. Cer. Soc., 60, pp. 520-525, (1977).

12. W. V. Cummings and D. E. Mahagin, "Crystallographic Changes in Fast-Reactor-Irradiated Boron Carbide," Trans. ANS, 17, pp. 187-88, (1973).

13. G. W. Hollenberg and B. Mastel, "Helium Bubbles in Irradiated Boron Carbide," American Ceramic Society Bulletin. 58 [3], p. 393 (1979).

14. A. H. Booth, A Method of Calculating Fission Gas Diffusion from UO_2 Fuel and Its Application to the X-2-f Loop Test, CRDC-721, Atomic Energy of Canada Ltd., 1957.

15. (R. O. Meyer), The Role of Fission Gas Release in Reactor Licensing, NRC Report, NUREG-75/077, November 1975.

16. J. C. Clayton, W. A. Bostrom, and F. C. Shrag, The Release of Helium from Slightly Irradiated Boron Carbide and Boron Carbide-Silicon Carbide Plates, WAPD-255, January 1962.

17. J. A. Turnbull, "The Distribution of Intragranular Fission Gas Bubbles in UO_2 During Irradiation," J. Nucl. Matl., 38, p. 204 (1971).

18. M. V. Speight, "A Calculation on the Size Distribution of Intragranular Bubbles in Irradiated UO_2," J. Nucl. Matl., 38, p. 236 (1971).

19. G. W. Greenwood, A. J. E. Foreman, and D. E. Rimmer, "The Role of Vacancies and Dislocations in the Nucleation and Growth of Gas Bubbles in Irradiated Fissile Material," J. Nucl. Matls., 4, p. 305 (1959).

20. D. R. Olander, Fundamental Aspects of Nuclear Reactor Fuel Elements, University of California, Berkely, Calif. TID-26711-P1, 1976.

21. G. W. Hollenberg and G. Walther, "The Elastic Modulus and Fracture of Boron Carbide," American Ceramic Society Bulletin, 58 [3] p. 328 (1979).

22. Nuclear Engineering Handbook, Harold Etherington, Ed., pp. 10-7, McGraw-Hill, New York (1956).

23. Handbook of Chemistry and Physics, Robert C. Weast, Ed., P. D-104, 47 edition, Chemical Rubber Co., Ohio (1967).

24. C. F. Williamson, etal., Tables of Range and Stopping Power of Chemical Elements for Charged Particles of Energy 0.5 to 500 MeV, CEA-R-3042 (1966).